

## STABILITY OF A SEMQ MICROPROBE: QUALITY CONTROL, QUANTITATIVE IMAGE ANALYSIS

E. D. Glover

The purchase of the SEMQ microprobe by the Department of Geology and Geophysics at the University of Wisconsin-Madison (UW) in 1981 was made for several reasons. The three spectrometers and six monochromators would allow counting nine elements simultaneously in the analysis of geological samples containing many elements; and, more important, the nine elements could be measured simultaneously in circumstances where automated probes are most valuable in the collection of line or area digital data (stage movement) with sufficient speed so as to cut job time to a minimum in multicomponent systems where accurate and precise data are desired. This paper describes control of the instrument for stability, production of, and transfer of data to a larger computer; and gives a number of examples to which such use has been put.

### *Instrument*

The automation of the stage, spectrometers, PHAs, and EDS system was provided by Tracor-Northern with the distinct advantage that the SEMQ is located only 5 miles away from Tracor-Northern's plant. We spent the first 2-3 years creating our own routines for analysis. Then extension to line and area digital scans was begun and schedules were written within the limited memory available to allow disk storage. We then copied other laboratories' practice of sending the data from the probe disk to a larger computer, in this case a 'Masscomp' system just coming up to routine operation as the (departmental) interactive system. This allowed the probe to be used as a probe, with the more manageable Masscomp UNIX system to be used for massaging, printing, graphing, plotting and tape storage (Table 1).

### *Initial Problems*

With the mechanics of collecting and organizing data into files set up and operating, attention was paid to the "quality control" aspect to check existing stability, and thus, time constraints limiting the system. A check was set up using Si K $\alpha$  measurement on any combination of the spectrometers; scanner #1, PET; scanner #2, ADP; and #9, ADP, a monochromator. The sample used was either silicon or silicon dioxide. An example of a successful run is shown in Fig. 1. Silicon was counted vs silicon as a standard. Correction by linear fit gave stable k ratios close to 1.0 on the three scanners. The mean and relative standard deviation

(r.s.d.) in % for the drift-corrected runs were (scanners 1, 2, and 9); 0.9963, 0.310; 1.0020, 0.325; 1.0016, 0.353 (well within the x-ray standard deviations 0.3 to 0.5%). After making a number of runs we found that it was necessary to check the filament behavior and to wait 1 to 2 h after sample entry for the vacuum to reach steady state. (Note conditions: Large sample chamber, but large diffusion pump with steady-state vacuum in the range of  $3 \times 10^{-6}$  Torr or less; sample chamber tie-in at 40  $\mu$ m.)

In check runs SiO $_2$  was used part of the time. These runs produced persistent "contamination" spots, which were used to produce a pattern giving quality control on the actual spatial distribution of the probed spots. Although the numbers on the x and y position dials read 10 $\mu$ m advancement, the pattern produced in Fig. 2 shows less accurate positioning of the sample. Since this pattern was repeatable we took care of this by simply defining a new space, SEMQ space. We are working on the conversion factors.

### *Application of Long Scans*

A series of applications of precise long scans are next presented. The development of the method and some of the applications have been made by the author. But many of the applications given are a part of the research and development of UW probe users; much of the probe work has been done by the researchers in collaboration with the author. The users results are presented here to illustrate the usefulness of the technique.

### *Study of a Waveguide Device*

This work by Kent Chocquette and Prof. Leon McCaughan is part of a study of Ti diffusion into Li-Niobate in waveguide devices. The measurement was made on an area covering an original section of a 5 $\mu$ m strip of Ti, scanning repeatedly across the strip along the length to establish the exact geometry. Counting times of 80 s helped gain precision at the low levels of Ti measured; k-ratios were collected and stored with a small correction made to the k-ratios measured (made from trial ZAF corrections). The scans are seen in Fig. 3, where several curves are superimposed. The goal of this work was to define the spatial precision of the diffused volume.<sup>1</sup>

### *Phase Diagram Determination*

A very broad application of quantitative line and image analysis has been made by Prof. Austin Chang at UW. He and his graduate students are interested in phase stability in

---

The author is at the University of Wisconsin (Geology and Geophysics), 1215 W. Dayton St., Madison, WI 63706.

TABLE 1.--The collection and transfer system was as follows:

Probe		RS-232		Masscomp	
Main Program	Schedule	Data			
Task	Cogrid	20 sample table(s) to Disk	840 byte string	Reconstituted table	Masscomp file
Flextran language - - - - -			- - - - C language - - - -		

multicomponent systems. Recently, they have been investigating phase stability of metallic contacts to GaAs with the use of diffusion couples. In Fig. 4 is shown a digital, linear scan over a diffusion couple of GaAs vs Ni. A simple overnight run can produce an atomic composition plot which shows directly the formation of GaAsNi<sub>3</sub>, with some variations, which the experimenter, Mr. X. Y. Zheng, can explain.

#### Modal or Phase Analysis

Many investigators have used stage or beam movement to count occurrences of phases present at grid locations to obtain the percentage of each phase. This method has been set up here for beam or stage movement; if the grid interval is reduced, the method gives quantitative image analysis. Present use at UW is mainly of line scans for checking concentration gradients to allow inference of P-T conditions of the formation process,<sup>2</sup> or to sort out chemical, structural, or orientation effects in minerals.

Figure 5 is a polarized light picture of a feldspar grain studied by Prof. L. G. Medaris. The superimposed Ca plot data shows that chemical effects are present. Because a focused electron beam and a 1µm interval were used, the Na value (which complements Ca) was variable since the heat produced causes Na mobility; however, the Ca and also the Al concentrations correlate directly with the extinction of the transmitted light by the crystal. There is a gradual increase of Ca and Al toward the center of the grain (right) and intermittent zones of high and low Ca and Al. This information with other data, allows assessment of the changes that have taken place in the development of the rock, as well as assessment of the chemical evolution of the magma from which the plagioclase has crystallized.

#### Homogeneity of NBS Glass K-411

The next sample, NBS Glass standard K-411, may be considered as a test for stability or a check on homogeneity. It started as a scan on a 30 × 30 grid, 5µm spacing. Only 14 of the 30 passes were made in a 9.5h time interval. Data on the means and standard deviations of four elements (two duplicated) are shown in Table 2 along with the x-ray standard deviations. All are close to the x-ray standard deviations except Fe on the two scanners measured. Both are

0.55 rather than the 0.34 and 0.38 calculated. Is K-411 inhomogeneous for Fe? A look at the curves (Fig. 6) shows a "bad" point with Fe high and the other elements low. Removal of this point produced the lower set of data (Table 2) in which all the standard deviations average less than 10% more than the x-ray values. The standard gets a clean bill of health except for one point (point 420) which has a high Fe content.<sup>3</sup>

#### Homogeneity of Nb-Ti Alloy

This research is part of a U.S. Department of Energy sponsored effort to create Nb-Ti wire composite for superconducting magnets for use in control of accelerators in high-energy physics. Taking part in the effort are Fermi National Accelerator Laboratory, Brookhaven Laboratory, Lawrence Berkeley Laboratory, the Applied Superconductivity Laboratory at UW, plus other laboratories, as well as manufacturers and processors. In spite of the sophisticated development of the superconducting composites of Nb-Ti, a basic problem has been the production of a reasonably homogeneous alloy to produce composites with maximum current capacity.<sup>4</sup> The measurement of this homogeneity has been carried out on the SEMQ by Peter Lee. This phase is only a small part of the total effort to develop the composite, but it is a basic one. What is shown here is the extremes of homogeneity development seen depending on the details of processing. The first plot (Fig. 7) shows a 400-point 10µm scan which was repeated after the first pass. The repetition is extraordinarily good; the two curves are hardly seen to separate. This sample is rather inhomogeneous and the curves demonstrate the spatial distribution. Figures 8 and 9 show successive improvement in the homogeneity. The collection of line scan data was usually sufficient. However, the technique was expanded in some cases to produce a quantitative image. A 50 × 32 grid with a 10µm interval is displayed contour-wise in Figs. 10, 11, and 12. This 37h run was drift-corrected to give (for all points) means and r.s.ds. of 0.5315, 0.56%; 0.4677, 0.48%; 0.992, 0.14% for Nb, Ti, and the total. In spite of the high precision, the contour maps show vividly the nonrandom distribution.

TABLE 2.--MEAN and R.S.D. of k-RATIOS of NBS GLASS K-411 (20 kV, 20 NA SAMPLE CURRENT, 20s COUNT, 5 $\mu$ m GRID).

element	mean	<u>r.s.d. %</u>	<u>r.s.d. %</u>	<u>x-ray r.s.d. %</u>
		<u>as taken</u>	<u>bad point omitted</u>	
Si1	1.0000	0.38	.37	.37
Si9	1.0004	0.71	.71	.63
Ca	.9992	0.31	.25	.25
Fe2	0.9997	0.55	.38	.34
Fe4	1.0037	0.55	.40	.38
Mg	1.0035	0.69	.66	.62

### Conclusions

In view of the data obtained in measurement on real systems several conclusions can be drawn. With steady-state vacuum and a well-behaved filament (properly installed), the present instrument gives high precision in measurements over a period up to 20 h (or more) with standardization only at the beginning and ends of the run. In the case of the NBS K-411 glass run on a 9.5h scan, the standard deviation was very little above the x-ray standard deviation. With the above conditions satisfied and with more frequent standardization, the precision could be routinely maintained at the x-ray standard deviation level. A very necessary condition for such precision is stable x-ray detection systems, including proportional counters and amplification. Proportional counters must be checked by such a long analysis run. If they consistently do not measure up they must be rejected. The accuracy of the stage movement on a micrometer scale can be checked by a grid pattern of contamination spots on a crystal such as quartz.

### References

1. L. McCaughan and K. D. Chocquette, "Origin of and solution to crosstalk in Ti:LiNbO<sub>3</sub> directional coupler switches," *J. Quantum Electronics* 22: 947-951, 1986.
2. L. G. Medaris and H. F. Wang, "A thermal-tectonic model for high-pressure rocks in the Basal Gneiss Complex of western Norway," *Lithos* 19: 299-315, 1986.
3. R. Marinenko, "Preparation and characterization of K-411 and K-412 mineral glasses for microanalysis: SRMA 70," *NBS Spec. Pub.* 260-74, 1982.
4. P. J. Lee and D. C. Larbelestier, "Microstructure development in a high current density NbTi superconducting composite," *Proc. 45th Ann. Meet. EMSA*, 1985.

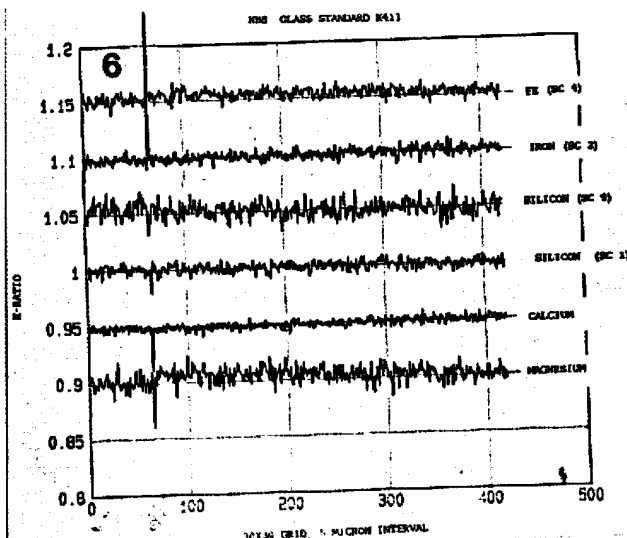
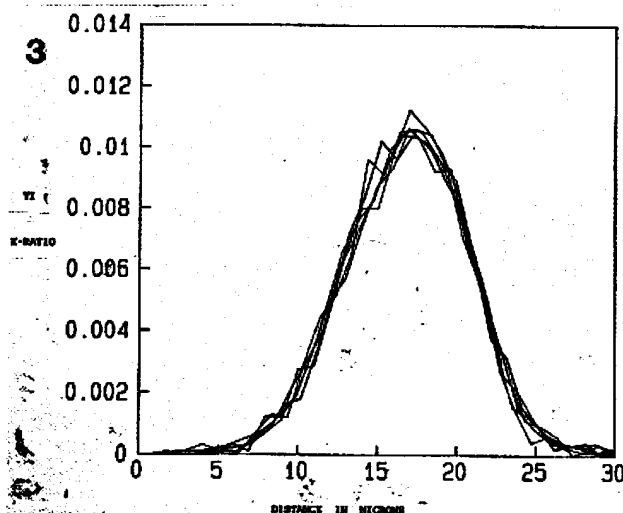
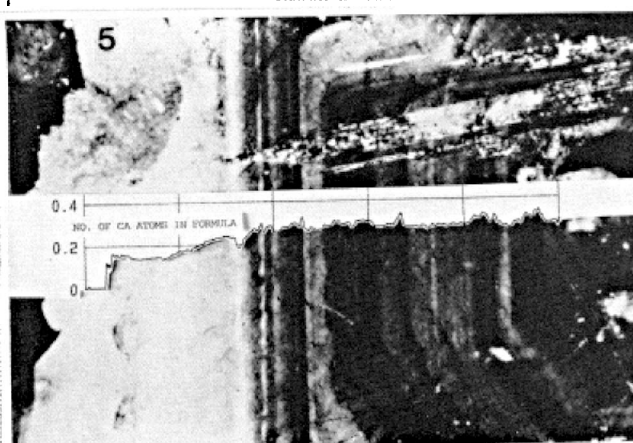
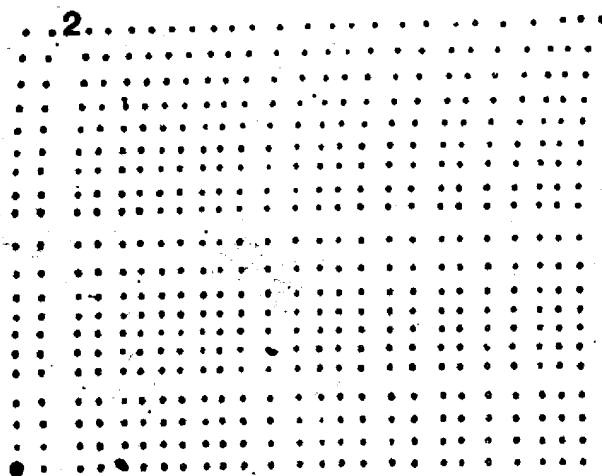
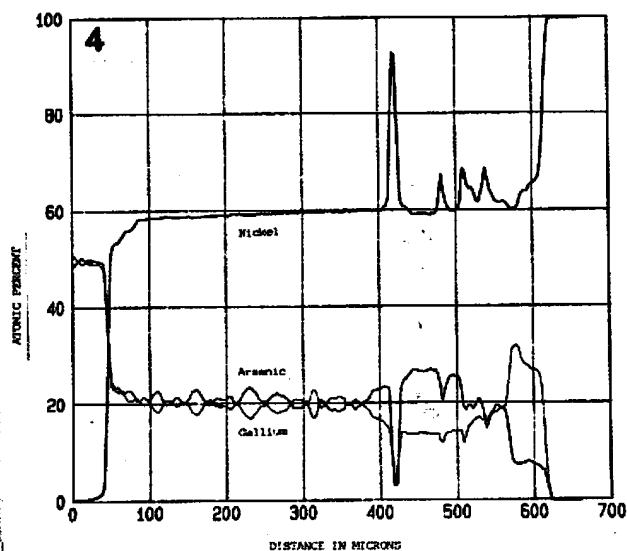
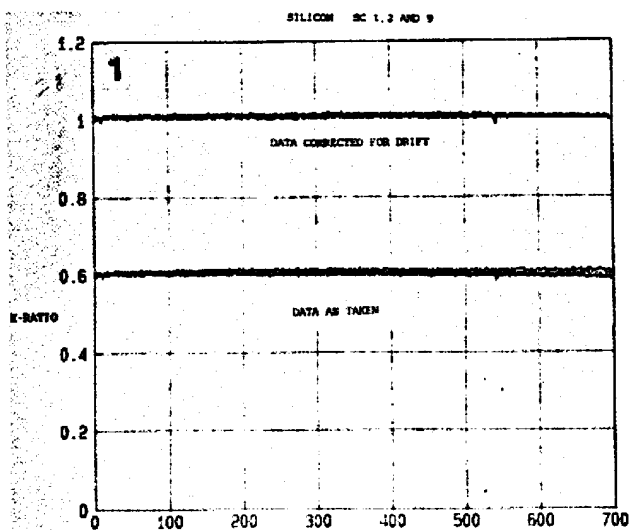


FIG. 1.--Silicon k-ratios for three scanners for a 700-point scan, 2 $\mu$ m interval, time  $\sim$ 12 h. Vertical scale is correct for upper curve/ lower curve is offset 0.4 unit.

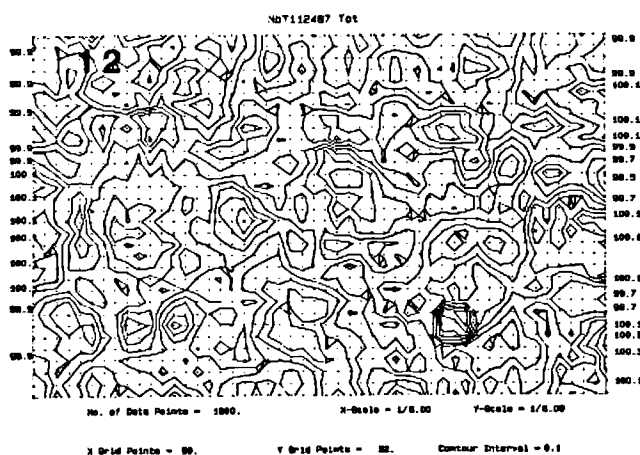
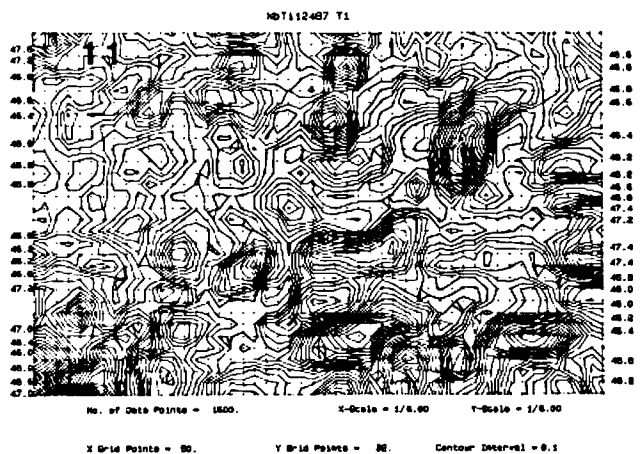
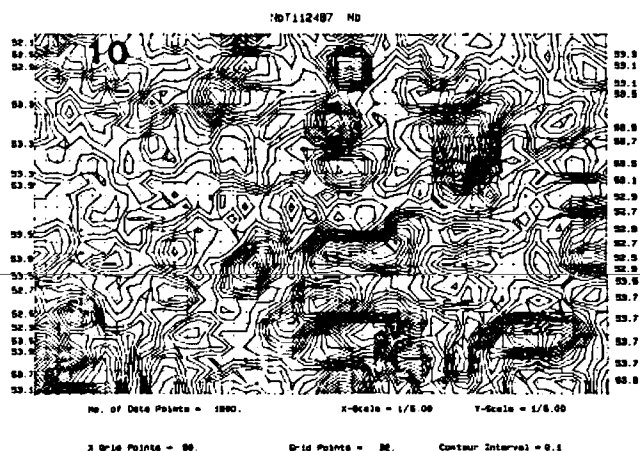
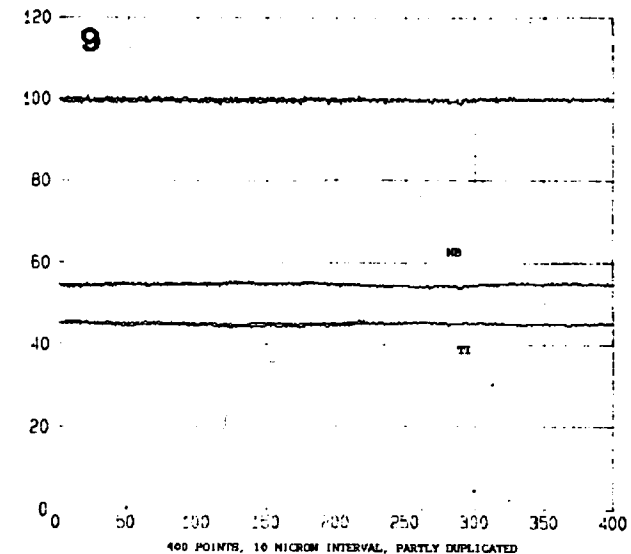
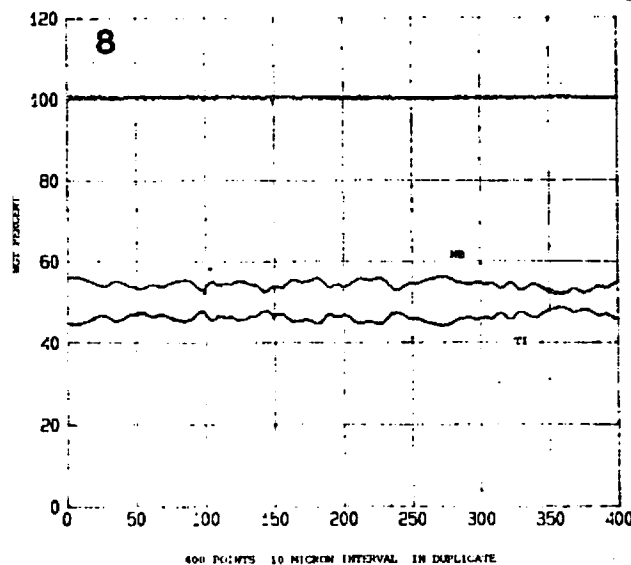
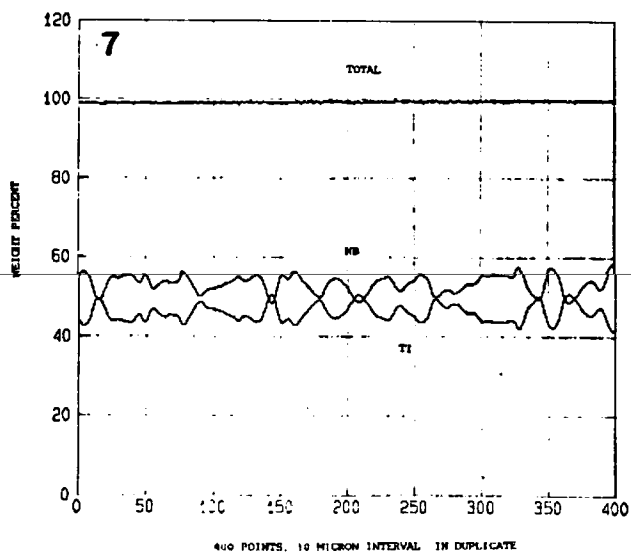
FIG. 2.--Position of the probe beam as stage moved over 10 $\mu$ m grid. Sample: quartz (SiO<sub>2</sub>), Hot Springs, Ark.

FIG. 3.--Plot of k-ratios of Ti across several traverses of Ti strip, 5  $\mu$ m wide  $\times$  670 Å thick, diffused into LiNbO<sub>3</sub>. Beam size 2  $\mu$ m; interval, 1  $\mu$ m.

FIG. 4.--Plot of atomic % of Ga, As, and Ni across diffusion boundary GaAs-Ni.

FIG. 5.--Superimposed plot of number of Ca atoms/formula [Na(Ca)Al(Al)<sub>2</sub>Si<sub>3</sub>(Si<sub>2</sub>)O<sub>8</sub>] on photo of plagioclase feldspar crystal (polarized light with crossed nicols). Scan length: 1000 points, 1 $\mu$ m interval.

FIG. 6.--Plot of k-ratios of Fe, Si, Ca, Mg in NBS K-411 glass over 5 $\mu$ m intervals. Vertical scale corresponds to Si(Sc 1). Other k-ratio curves are offset by multiple of 0.05 unit.



FIGS. 7,8,9.--Three (duplicated) linear scans on NbTi alloys of increasing homogeneity (wgt. % vs successive points at 10µm intervals).  
FIGS. 10,11,12.--Contour map of Nb,Ti and total concentration (wgt %) of 50 × 32, 10µm grid of NbTi alloy giving quantitative image with 10µm resolution.